

## Electronic Supplementary Information

### Hybridized local and charge-transfer excitation in 2,5-substituted D-A type siloles for efficient OLEDs

Liang Zhang,<sup>‡a</sup> Linzhong Wang,<sup>‡b</sup> Kerim Samedov,<sup>\*‡a</sup> Mingxing Chen,<sup>c</sup> Dongcheng Chen<sup>\*b</sup>  
and Yuanjing Cai<sup>\*a</sup>

<sup>a</sup> Beijing Advanced Innovation Center for Soft Matter Science and Engineering, Beijing University of Chemical Technology, Beijing, 100029 P. R. China. E-mail: kerim.samedov@hotmail.com; gardencyj@mail.buct.edu.cn

<sup>b</sup> State Key Laboratory of Luminescent Materials and Devices, Institute of Polymer Optoelectronic Materials and Devices, South China University of Technology, Guangzhou, 510640 P. R. China. E-mail: mschendc@scut.edu.cn

<sup>c</sup> Analytical Instrumentation Center, Peking University, Beijing, 100871 P. R. China.

<sup>‡</sup> These authors contribute equally to this work.

---

## Materials and Characterization Methods

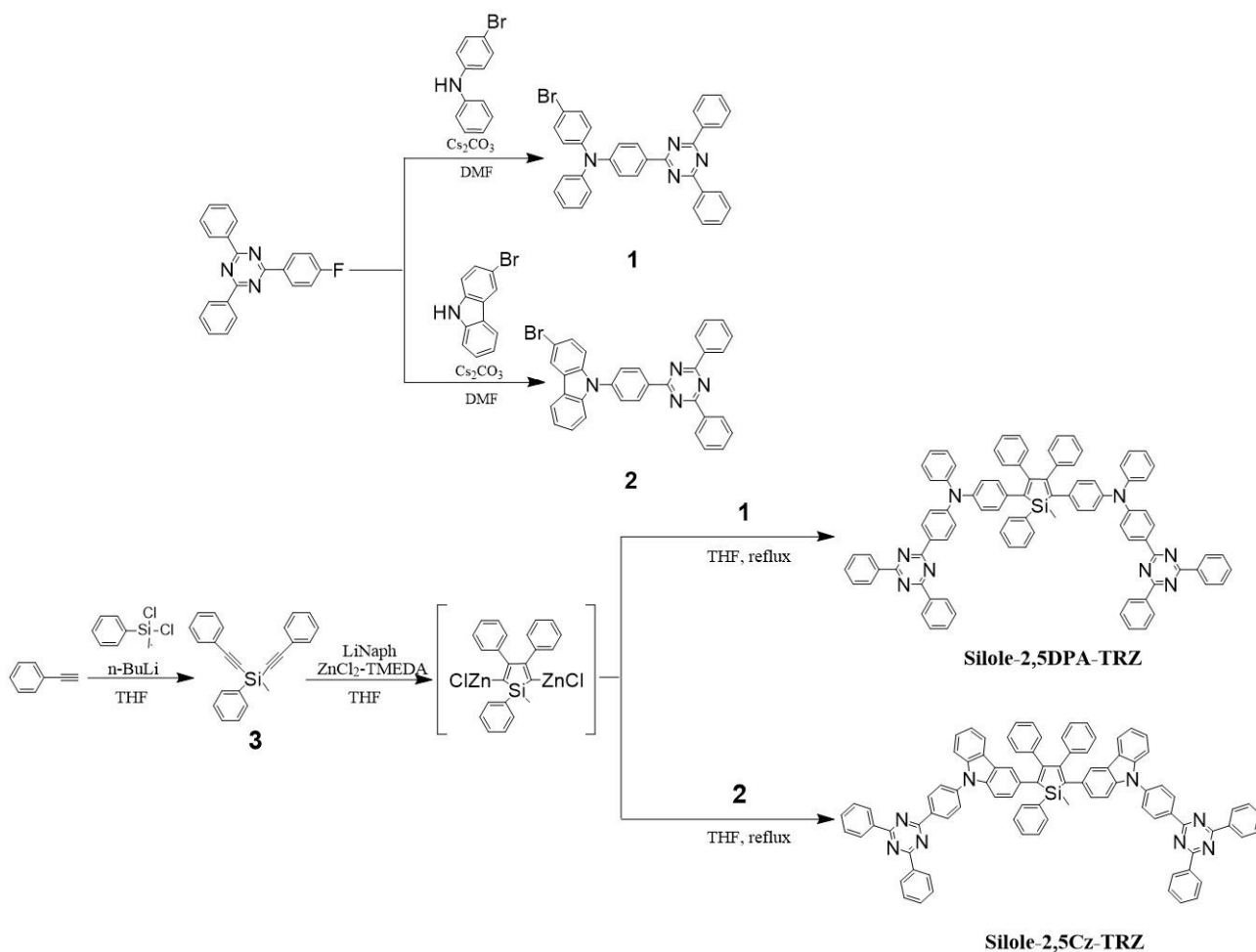
Unless otherwise stated, all chemicals and reagents were purchased from Sigma Aldrich and used without further purification. THF was distilled from sodium benzophenone ketyl radical directly before use in an oxygen-free argon atmosphere. Compounds **1**, **2** and **3** were synthesized according to the methods described in the literature.  $^{1-3}$   $^1\text{H}$  and  $^{13}\text{C}\{^1\text{H}\}$  NMR spectra were measured on a Bruker AVANCE III spectrometer in deuterated chloroform ( $\text{CDCl}_3$ ) using tetramethylsilane (TMS;  $\delta = 0$ ) as the internal reference. Mass spectra were recorded on an AXIMA-performance MA mass spectrometer operating in a MALDI-TOF mode. Thermogravimetric analyses (TGA) were conducted on STA7300 under  $\text{N}_2$  atmosphere with a heating rate of  $10^\circ\text{C min}^{-1}$ . Differential Scanning Calorimetry (DSC) analyses were carried out using TA instrument under a nitrogen atmosphere with a heating rate of  $10^\circ\text{C min}^{-1}$ .

*Cyclic voltammetry measurements:* CV of **Silole-2,5-DPA-TRZ** and **Silole-2,5-Cz-TRZ** in DCM were carried out on an electrochemical workstation CHI 660E using tetra-n-butylammonium hexafluorophosphate ( $\text{TBAPF}_6$ , 0.1 M in DCM) as the electrolyte, platinum as the counter electrode, and Ag/AgCl as the reference electrode (versus ferrocene  $\text{Fc}/\text{Fc}^+$ ). The resulting HOMO/LUMO values were calculated according to the equation (unit: eV)  $E_{\text{HOMO}} = -(E_{\text{ox}} - E_{\text{Fc}/\text{Fc}^+} + 4.8)$ ,  $E_{\text{LUMO}} = E_{\text{HOMO}} + E_{\text{g}}$ , where  $E_{\text{g}}$  is determined from the UV-vis absorption spectrum.

*Photophysical measurements:* UV-vis spectra were recorded on a Shimadzu UV-3600 spectrophotometer using 1.5 cm path-length quartz cells. All film samples were made on quartz glasses with an area of  $1.5\text{ cm} \times 1.5\text{ cm}$ . Photoluminescence tests were measured on an Edinburgh F-1000 spectrofluorometer with steady and transient modes. PL quantum yields were recorded on an FLS-980 spectrometer equipped with a calibrated integrating sphere. PL spectra were obtained with a Xenon light source. Fluorescence lifetimes were measured using a 390 nm picosecond pulsed light-emitting diode excitation source. The photophysical properties of the samples in solution were tested by determining the emission and absorption wavelengths of the samples in different solvents. The  $\Delta E_{\text{ST}}$  ( $= E_{\text{S}_1} - E_{\text{T}_1}$ ) is determined by the fluorescence and phosphorescence spectra, in which the energy of  $\text{S}_1$  can be calculated from the onset of the fluorescence spectrum ( $E_{\text{S}_1} = 1240/\lambda_{\text{onset}}$ ), and the phosphorescence spectrum at 77 K clearly indicates the  $\text{T}_1$  which can be derived from the  $E_{0-0}$  band. <sup>[4-6]</sup>

*Device fabrication and characterization:* The purchased ITO glass was used as the substrate after having been carefully cleaned with isopropyl alcohol, acetone, toluene and deionized water, then going through a drying procedure at  $120^\circ\text{C}$  in an oven and UV-zone treatment. The sheet resistance of the ITO glass is  $20\ \Omega\ \text{square}^{-1}$ . The prepared ITO glasses were transferred to the deposition system in the glove box under vacuum. All the organic layers were deposited at a rate of  $1.0\ \text{\AA}\ \text{s}^{-1}$ , the deposition rates for cathode LiF and the Al metal layer were  $0.1\ \text{\AA}\ \text{s}^{-1}$  and  $4.0\ \text{\AA}\ \text{s}^{-1}$ . The device performance and electroluminescent (EL) spectra were measured under ambient conditions at room temperature, using the Electroluminescence Efficiency Measurement system XP-EQE-Adv. The active device area was  $3\text{ mm} \times 3\text{ mm}$ .

## Synthesis characterization



**Scheme S1.** Synthetic routes to **Silole-2,5DPA-TRZ** and **Silole-2,5Cz-TRZ**

### Synthesis of compound 1

Under nitrogen atmosphere, to a 250 mL two-necked flask was added 4-bromophenylamine (2.55 g, 10.20 mmol), cesium carbonate (16.3 g, 50.00 mmol), anhydrous oxygen-free DMF (100 mL). The resulting solution was stirred at room temperature for 30 min, and then 2-(4-fluorophenyl)-4,6-diphenyl-1,3,5-triazine (3.34 g, 10.20 mmol) was added. The reaction solution was stirred overnight at 155 °C. After the reaction was completed, the reaction solution was cooled to room temperature and then quenched with deionized water. Then the raw product was extracted with dichloromethane and the organic layer was washed three times with water (80 mL). The organic layer was dried over anhydrous magnesium sulfate. After filtration, the solvent was removed under reduced pressure, and the residue was purified by flash chromatography on a silica gel column using dichloromethane/petroleum ether (volume ratio: 1/5) to give **1** as a yellow solid (2.32 g, yield: 41%). <sup>1</sup>H NMR (400 MHz, 295 K, CDCl<sub>3</sub>, TMS, ppm): δ = 8.79-8.71 (d, 4H, Ar-*H*), 8.66-8.59 (d, 2H, Ar-*H*),

---

7.66-7.51 (m, 6H, Ar-*H*), 7.46-7.39 (d, 2H, Ar-*H*), 7.38-7.31 (m, 2H, Ar-*H*), 7.23-7.12 (m, 5H, Ar-*H*), 7.10-7.03 (m, 2H, Ar-*H*).  $^{13}\text{C}\{^1\text{H}\}$  NMR (101 MHz, 295 K,  $\text{CDCl}_3$ , TMS, ppm):  $\delta$  = 171.52, 171.15, 151.46, 146.67, 146.24, 136.55, 132.66, 132.50, 130.43, 129.81, 129.61, 129.02, 128.73, 126.82, 125.84, 124.71, 121.61, 116.70.

### Synthesis of compound 2

Under nitrogen atmosphere, to a 250 mL two-necked flask was added 3-bromocarbazole (2.59 g, 10.20 mmol), cesium carbonate (16.3 g, 50.00 mmol), anhydrous oxygen-free DMF (100 mL). The resulting solution was stirred at room temperature for 30 min, and then 2-(4-fluorophenyl)-4,6-diphenyl-1,3,5-triazine (3.34 g, 10.20 mmol) was added. The reaction solution was stirred at 155 °C overnight. After the reaction was completed, the reaction solution was cooled to room temperature and then quenched with deionized water. Then the raw product was extracted with dichloromethane/water three times and the organic layer was dried over anhydrous magnesium sulfate. After filtration, the solvent was removed under reduced pressure, and the residue was purified by flash chromatography on a silica gel column using dichloromethane/petroleum ether (volume ratio: 1/5) to give **2** as a white solid (3.69 g, yield: 65%).  $^1\text{H}$  NMR (400 MHz, 295 K,  $\text{CDCl}_3$ , TMS, ppm):  $\delta$  = 9.06-9.00 (m, 2H, Ar-*H*), 8.85-8.79 (m, 4H, Ar-*H*), 8.30-8.26 (m, 1H, Ar-*H*), 8.15-8.09 (d, 1H, Ar-*H*), 7.81-7.75 (d, 2H, Ar-*H*), 7.69-7.58 (m, 6H, Ar-*H*), 7.57-7.51 (m, 2H, Ar-*H*), 7.51-7.45 (m, 1H, Ar-*H*), 7.44-7.40 (m, 1H, Ar-*H*), 7.38-7.31 (t, 1H, Ar-*H*).  $^{13}\text{C}\{^1\text{H}\}$  NMR (101 MHz, 295 K,  $\text{CDCl}_3$ , TMS, ppm):  $\delta$  = 172.00, 170.98, 141.23, 140.95, 139.30, 136.25, 135.50, 132.86, 130.89, 129.17, 128.99, 128.88, 127.06, 126.84, 125.66, 123.34, 122.82, 120.95, 120.77, 113.32, 111.56, 110.29.

### Synthesis of compound 3<sup>0</sup>

Phenylacetylene (1.65 mL, 15.02 mmol) was dissolved in dry THF (50 mL) under a nitrogen atmosphere, cooled down to -78 °C with a dry ice/acetone cold bath, and *n*-butyl lithium solution in hexanes (9.0 mL, 18.00 mmol) was added dropwise to the solution. The mixture was stirred for 3 h at -78 °C, and then dichloromethylphenylsilane (1.20 mL, 7.28 mmol) was added to the solution. The reaction mixture was allowed to stir overnight at -78 °C under a nitrogen atmosphere. After that, the reaction mixture was warmed up to room temperature and quenched with concentrated hydrochloric acid (37%, ca. 6 mL) and water (ca. 30 mL). After stirring for 30 minutes at room temperature the quenched reaction mixture was extracted with ethyl acetate three times, and the organic layers were combined and dried over magnesium sulfate. After filtration, the solvent was removed, and the residue was purified by flash chromatography on a silica gel column using dichloromethane/petroleum ( $v/v = 1:9$ ) as eluent to give **3** a white powder (1.66 g, 70.1%).  $^1\text{H}$  NMR (400

MHz, CDCl<sub>3</sub>, δ (TMS, ppm)) 7.86-7.84 (m, 2H), 7.55-7.53 (m, 4H), 7.44-7.42 (m, 3H), 7.34-7.28 (m, 6H), 0.71 (s, 3H). <sup>13</sup>C{<sup>1</sup>H} NMR (400 MHz, CDCl<sub>3</sub>, δ (TMS, ppm)) 134.28, 132.32, 130.21, 129.17, 128.36, 128.21, 122.62, 107.55, 89.17, 0.27.

### Synthesis of Silole-2,5DPA-TRZ

A solution of lithium naphthalenide (LiNaph) was prepared by stirring a mixture of naphthalene (1.28 g, 10.00 mmol) and lithium granules (69 mg, 10.00 mmol) in dry THF (63 mL) for 3 h at room temperature under nitrogen atmosphere. A solution compound **3** (0.80 g, 2.50 mmol) in THF (25 mL) was added dropwise to the solution of LiNaph, and the reaction mixture was stirred for 1 h at room temperature. After that, the reaction mixture was cooled down to -10 °C, and ZnCl<sub>2</sub>-TMEDA (3.21 g, 12.50 mmol) in THF (63 mL) was added. A fine suspension formed. It was stirred for 1 h at room temperature and then Pd(PPh<sub>3</sub>)<sub>2</sub>Cl<sub>2</sub> (0.11 g, 0.16 mmol) and compound **1** (3.34 g, 6.00 mmol) were added and the reaction mixture was refluxed overnight. The next day, the reaction mixture was cooled to room temperature and quenched with ca. 1.0 M hydrochloric acid. The quenched reaction mixture was then poured into water and extracted with dichloromethane. The organic layer was separated and dried over magnesium sulfate. After filtration, the solvent was removed, and the residue was purified by silica gel column chromatography using dichloromethane/petroleum (v/v = 1/1) as eluent to yield **Silole-2,5-DPA-TRZ** as an orange powder (0.55 g, 28.5%). <sup>1</sup>H NMR (400 MHz, CDCl<sub>3</sub>, δ (TMS, ppm)): δ = 8.74-8.72 (m, 8H), 8.56-8.54 (m, 4H), 7.76-7.74 (m, 2H), 7.60-7.52 (m, 15H), 7.44-7.41 (m, 3H), 7.29-7.27 (m, 3H), 7.11-7.06 (m, 15H), 6.96-6.93 (m, 4H), 6.81 (m, 7H), 0.89 (s, 3H). <sup>13</sup>C{<sup>1</sup>H} NMR (400 MHz, CDCl<sub>3</sub>, δ (TMS, ppm)): δ = 171.44, 171.21, 155.61, 151.75, 146.79, 144.48, 139.55, 139.02, 136.63, 134.98, 134.78, 134.20, 132.43, 131.26, 130.25, 129.99, 129.56, 129.01, 128.91, 128.70, 128.52, 127.85, 126.63, 125.92, 124.45, 124.32, 121.40, 119.16, -5.76. MS (MALDI-TOF) m/z: calcd for C<sub>89</sub>H<sub>64</sub>N<sub>8</sub>Si, 1272.50 found [M+H]<sup>+</sup>1273.4866.

### Synthesis of Silole-2,5Cz-TRZ

A solution of lithium naphthalenide (LiNaph) was prepared by stirring a mixture of naphthalene (1.28 g, 10.00 mmol) and lithium granules (69 mg, 10.00 mmol) in dry THF (63 mL) for 3 h at room temperature under nitrogen atmosphere. A solution of compound **3** (0.80 g, 2.50 mmol) in THF (25 mL) was added dropwise to the solution of LiNaph, and the reaction mixture was stirred for 1 h at room temperature. After that, the reaction mixture was cooled down to -10 °C, and ZnCl<sub>2</sub>-TMEDA (3.21 g, 12.50 mmol) in THF (63 mL) was added. A fine suspension formed. It was stirred for 1 h at room temperature and then Pd(PPh<sub>3</sub>)<sub>2</sub>Cl<sub>2</sub> (0.11 g, 0.16 mmol) and compound **2** (3.31 g, 6.00 mmol) were added and the reaction mixture was refluxed overnight. The next day, the reaction mixture was cooled to room temperature and quenched with ca. 1.0 M hydrochloric acid. The quenched reaction mixture was then poured into water, extracted with dichloromethane, and dried over magnesium sulfate. After filtration, the solvent was removed, and the residue was purified by flash silica gel column chromatography using dichloromethane/petroleum (v/v = 1:1) as eluent to yield **Silole-2,5-Cz-TRZ** as an orange powder (0.56 g, 25.4%). <sup>1</sup>H NMR (400 MHz, CDCl<sub>3</sub>, δ (TMS, ppm)): δ = 8.96-8.94 (m, 4H), 8.81-8.79 (m, 8H), 7.84-7.82 (m, 2H), 7.77-7.72 (m, 6H), 7.67-7.66 (m, 2H), 7.63-7.57 (m, 12H), 7.54-7.48 (m, 2H), 7.42-7.41 (m, 3H), 7.39-7.35 (m, 2H), 7.24-7.20 (m, 4H), 7.11-7.09 (m, 6H), 7.05-

7.02 (m, 6H), 0.98 (s, 3H).  $^{13}\text{C}\{^1\text{H}\}$  NMR (100 MHz,  $\text{CDCl}_3$ ,  $\delta$  (TMS, ppm)):  $\delta = 171.90, 171.04, 154.96, 141.76, 140.62, 139.90, 139.81, 138.74, 136.30, 134.98, 134.79, 134.54, 132.77, 132.07, 130.65, 130.33, 130.03, 129.15, 128.84, 128.48, 128.22, 127.92, 126.52, 126.46, 126.07, 124.10, 123.68, 120.95, 120.47, 120.29, 110.02, 109.53, -5.56$ . MS (MALDI-TOF)  $m/z$ : calcd for  $\text{C}_{89}\text{H}_{60}\text{N}_8\text{Si}$ , 1268.47; found  $[\text{M}+\text{H}]^+$  1269.5238.

### $^1\text{H}/^{13}\text{C}$ NMR spectra

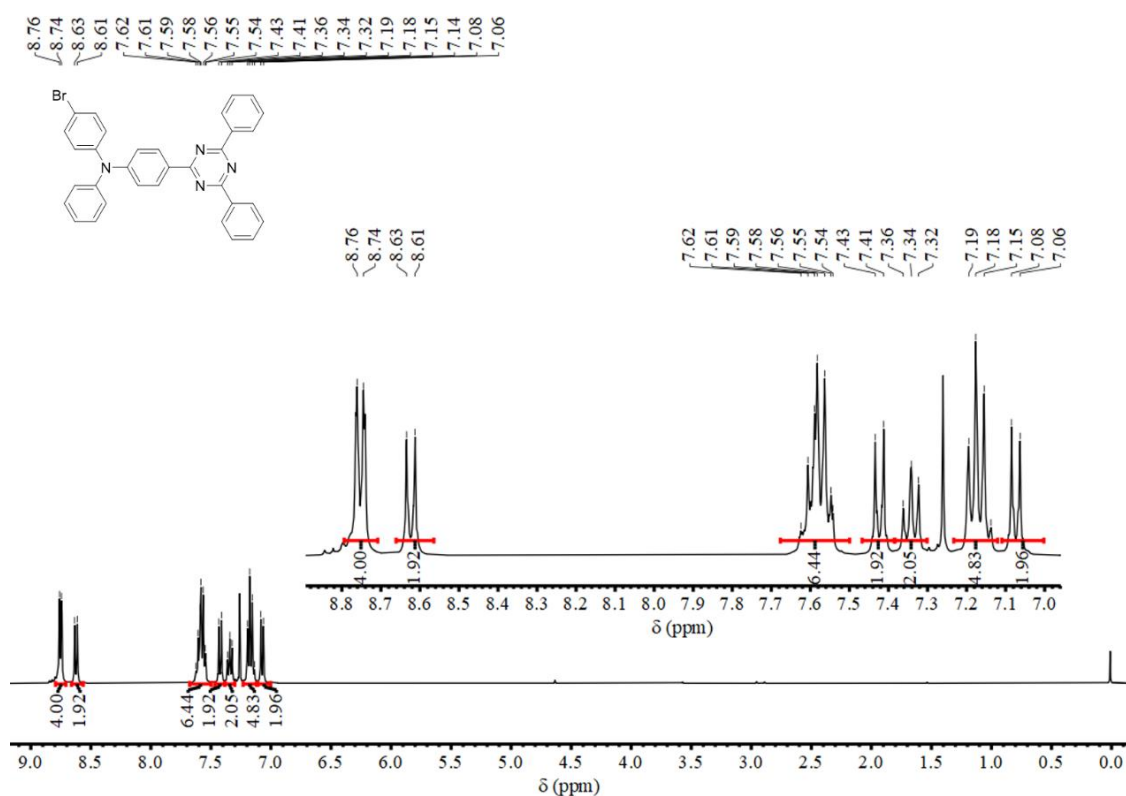
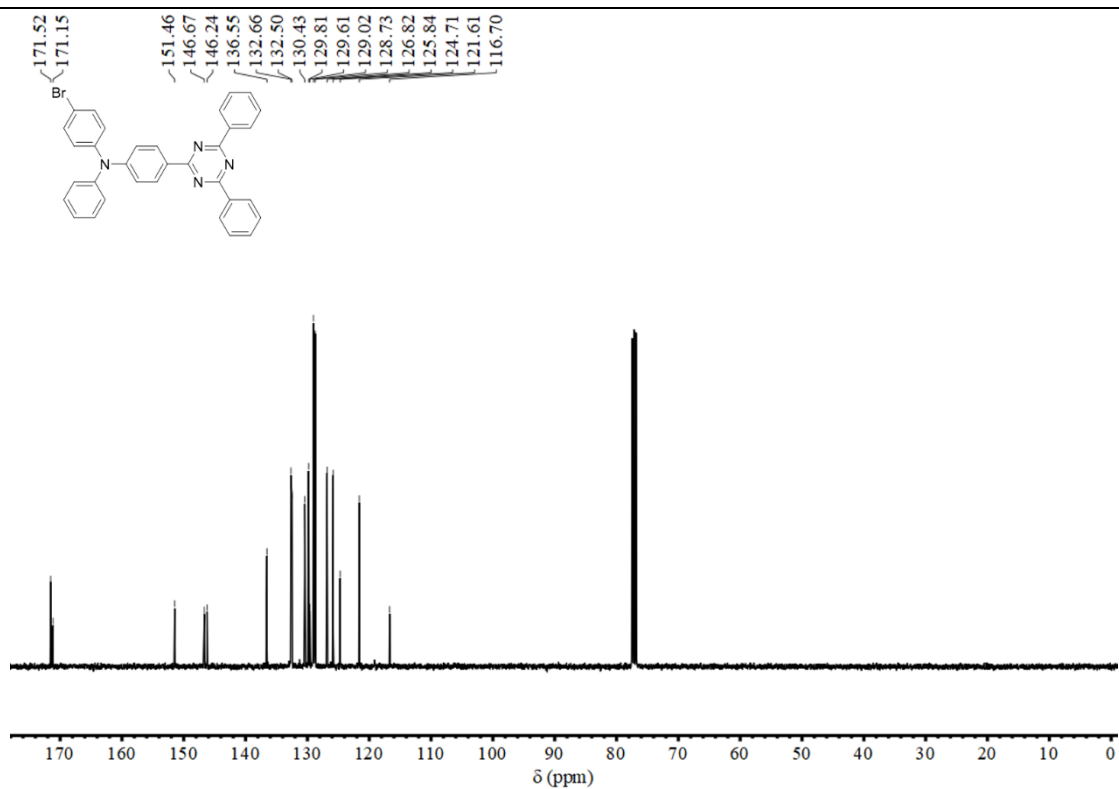
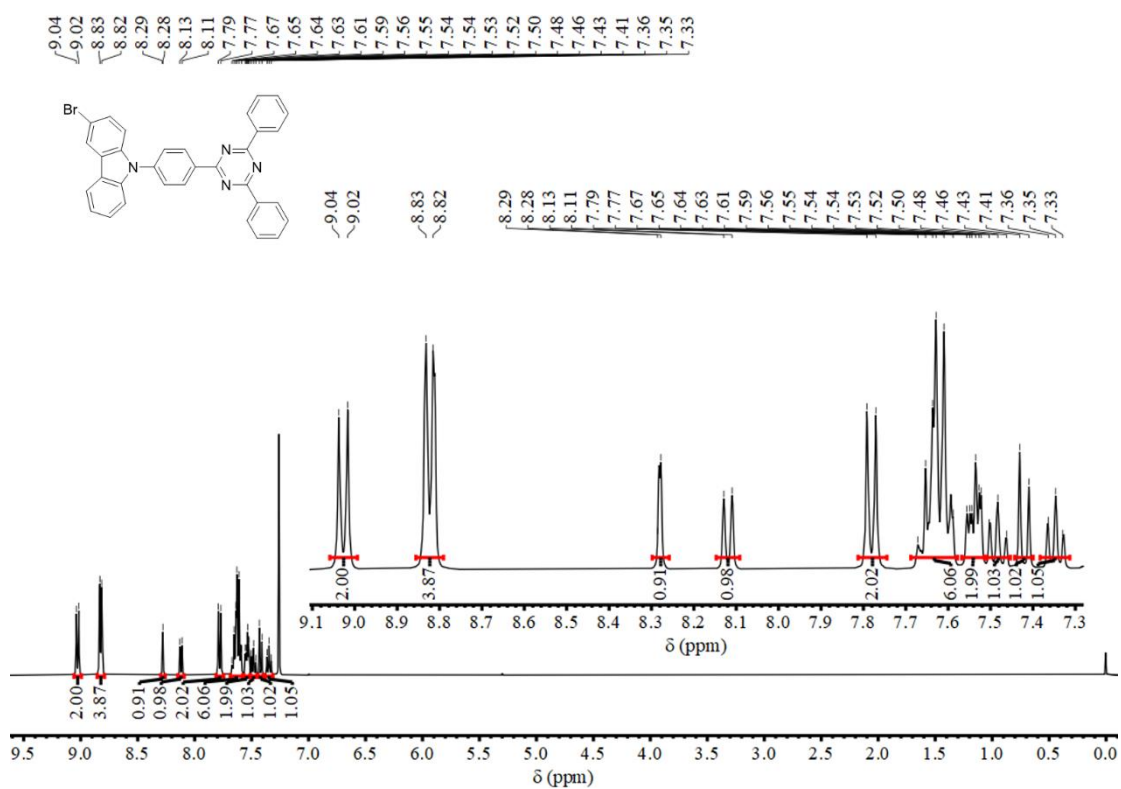


Figure S1.  $^1\text{H}$  NMR spectrum of compound **1** (400 MHz, in  $\text{CDCl}_3$ )



**Figure S2.**  $^{13}\text{C}\{^1\text{H}\}$  NMR spectrum of compound **1** (101 MHz, in  $\text{CDCl}_3$ ).



**Figure S3.**  $^1\text{H}$  NMR spectrum of compound **2** (400 MHz, in  $\text{CDCl}_3$ )

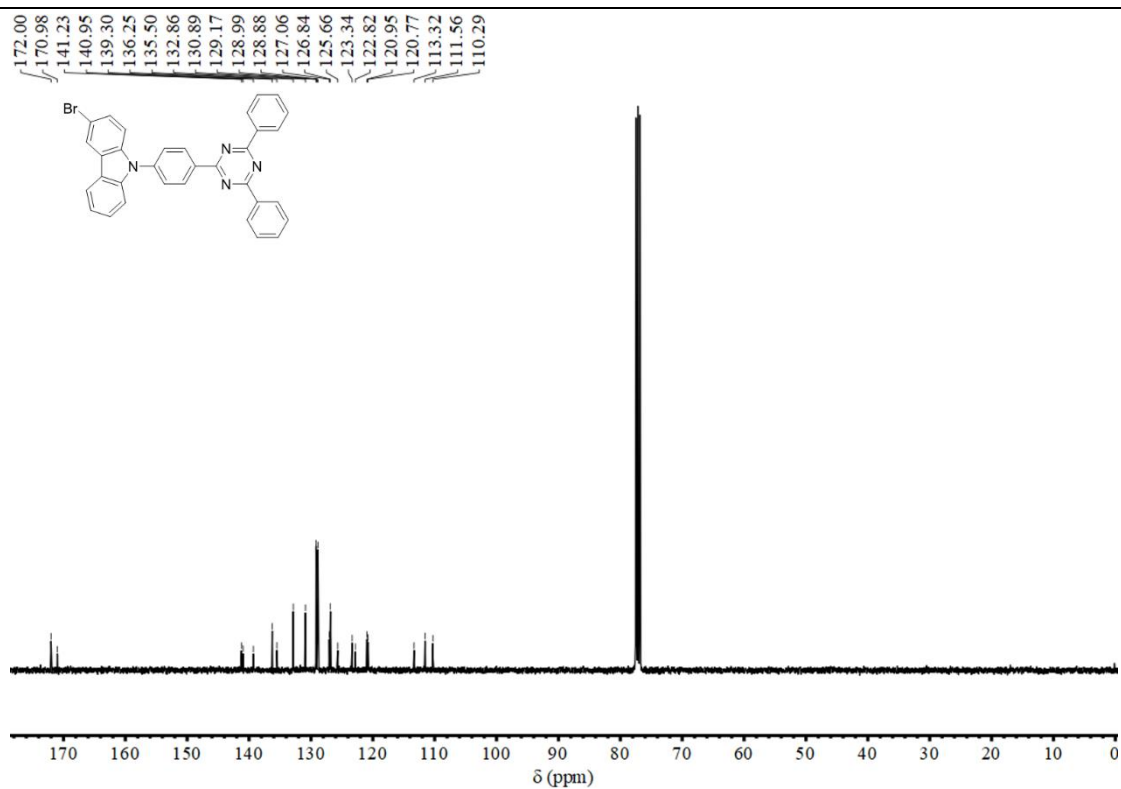


**Figure S4.**  $^{13}\text{C}\{^1\text{H}\}$  NMR spectrum of compound **2** (101 MHz, in  $\text{CDCl}_3$ ).

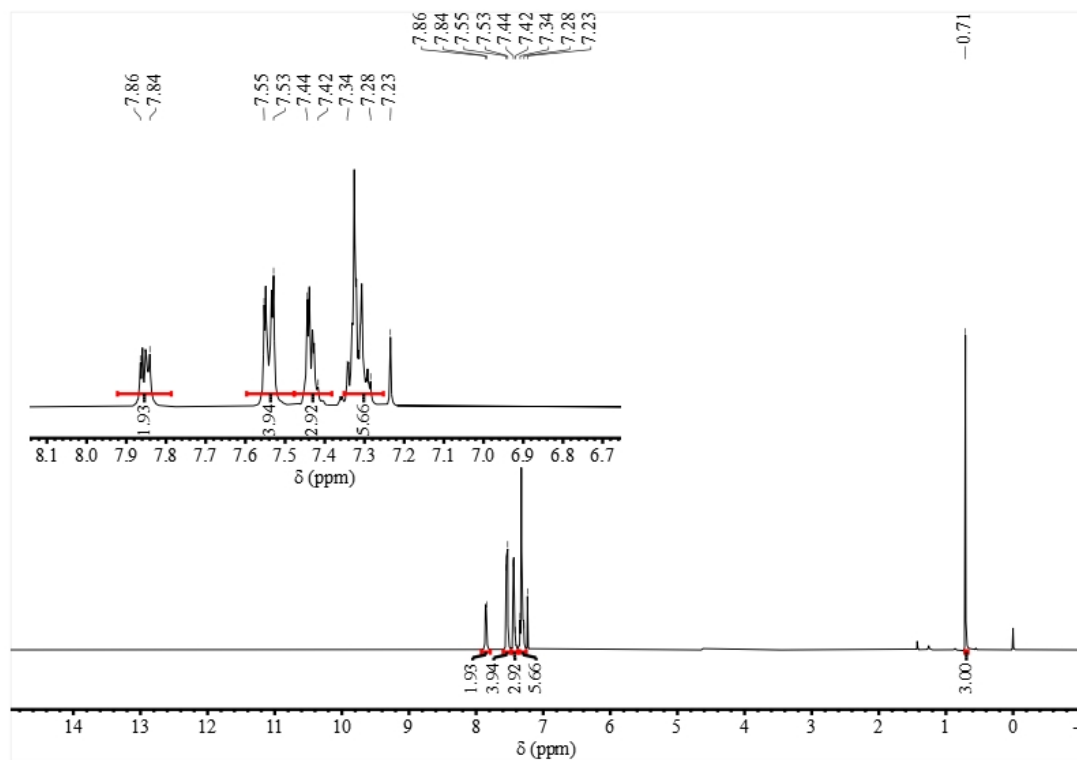


**Figure S5.**  $^1\text{H}$  NMR spectrum of compound **3** (400 MHz, in  $\text{CDCl}_3$ )

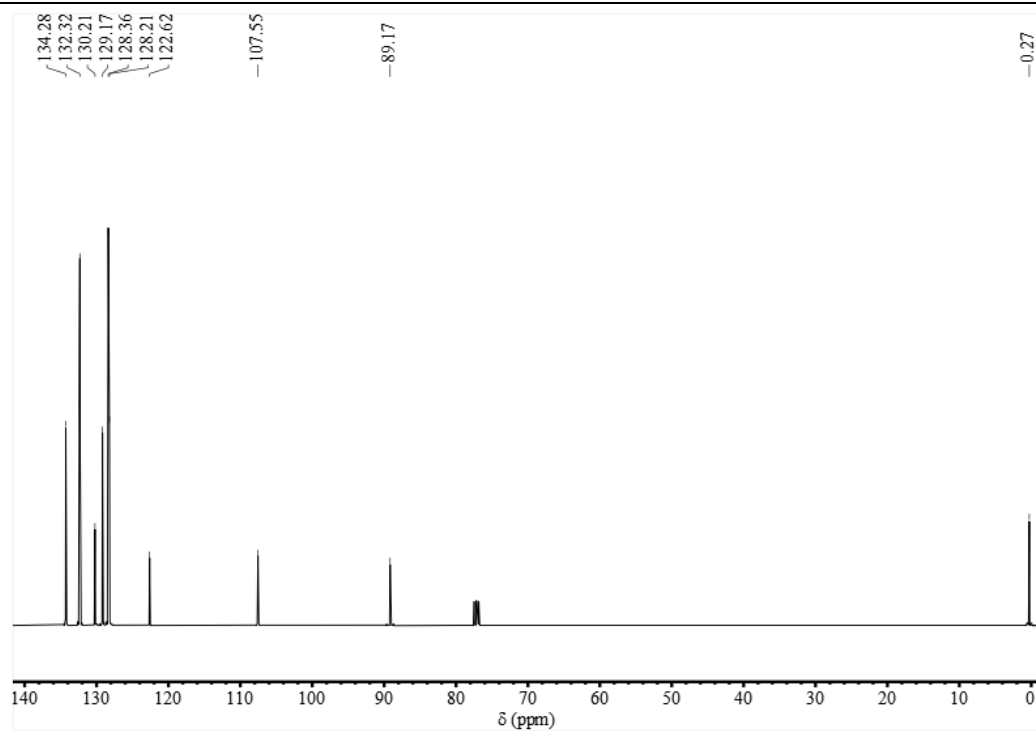


**Figure S6.**  $^{13}\text{C}\{^1\text{H}\}$ NMR spectrum of compound **3** (101 MHz, in  $\text{CDCl}_3$ ).

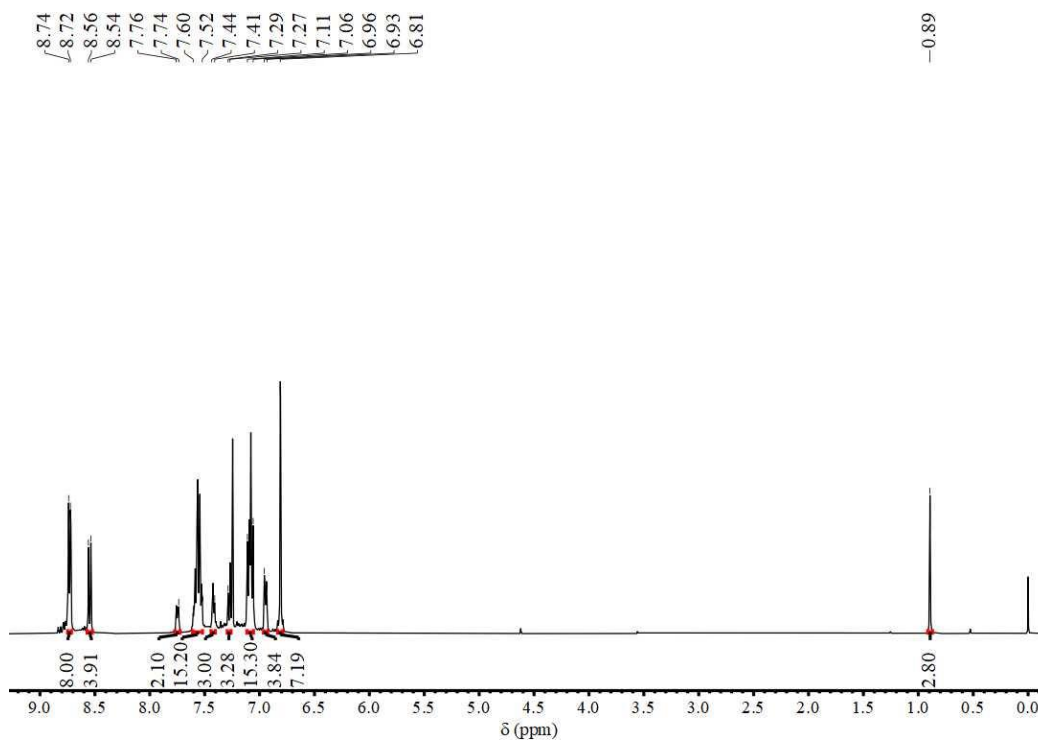


**Figure S7.**  $^1\text{H}$  NMR spectrum of compound **Silole-2,5DPA-TRZ** (400 MHz, in  $\text{CDCl}_3$ )

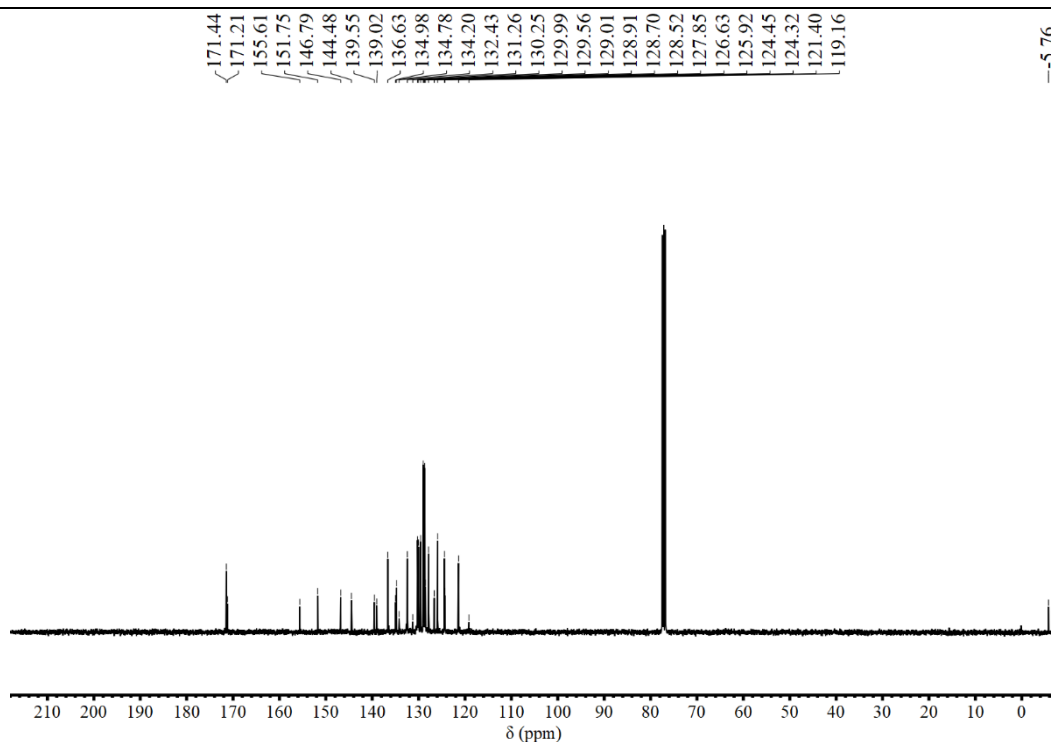


**Figure S8.**  $^{13}\text{C}\{^1\text{H}\}$ NMR spectrum of compound **Silole-2,5-DPA-TRZ** (101 MHz, in  $\text{CDCl}_3$ ).

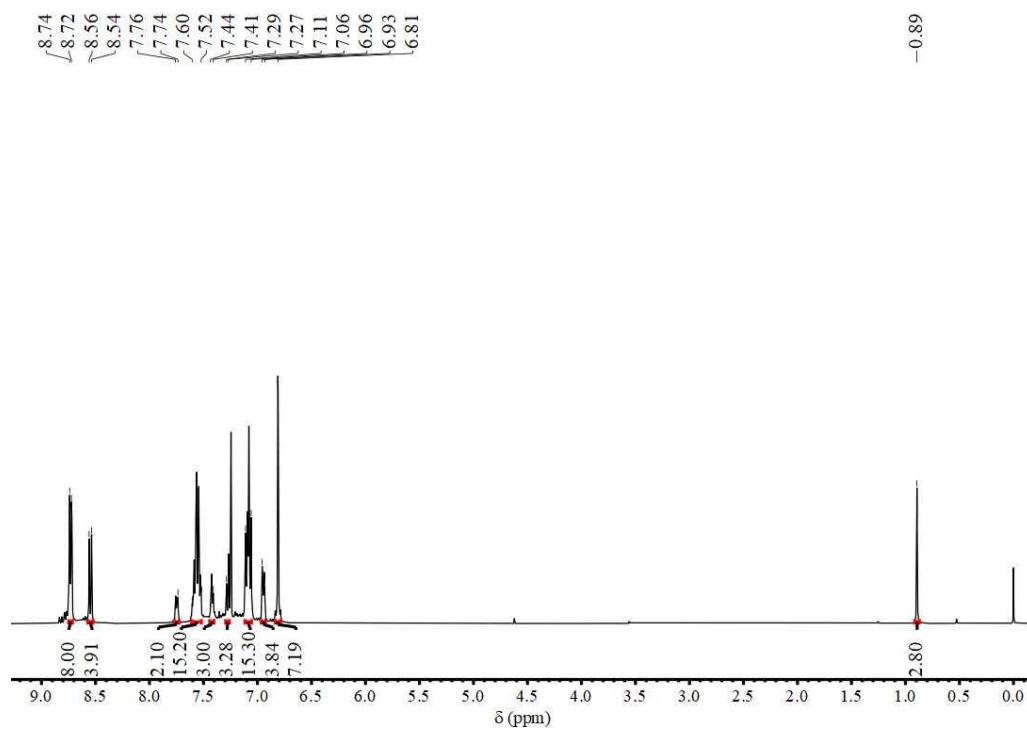


**Figure S9.**  $^1\text{H}$  NMR spectrum of compound **Silole-2,5Cz-TRZ** (400 MHz, in  $\text{CDCl}_3$ )

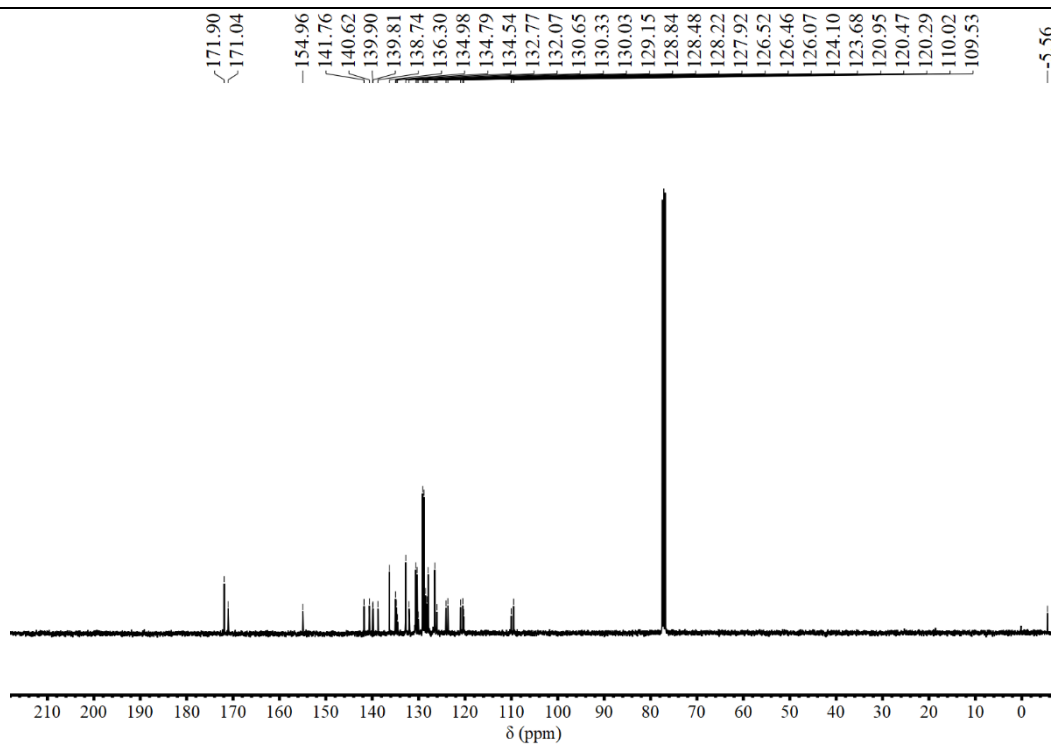


**Figure S10.**  $^{13}\text{C}\{^1\text{H}\}$  NMR spectrum of compound **Silole-2,5-Cz-TRZ** (101 MHz, in  $\text{CDCl}_3$ ).

### MALDI-TOF spectra

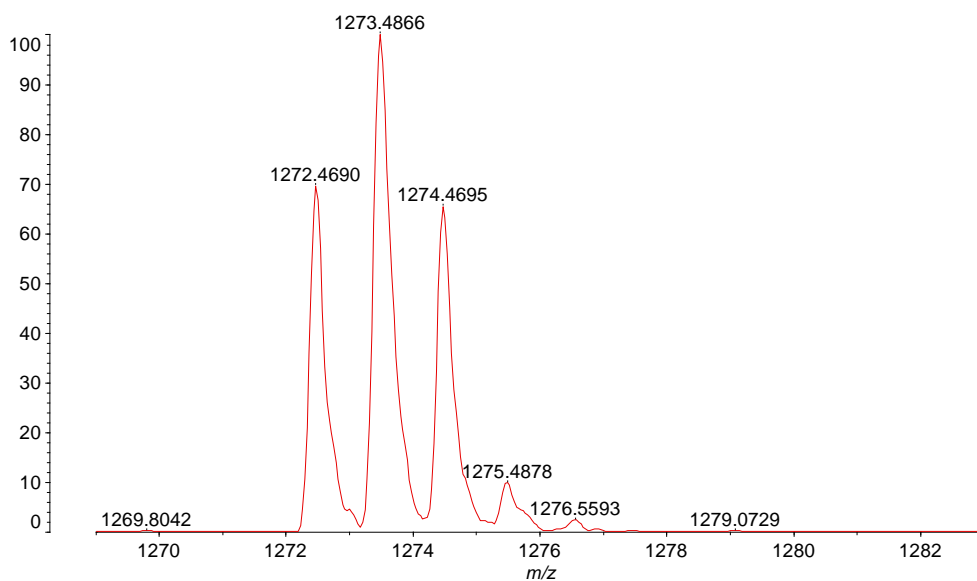


**Figure S11.** MALDI-TOF spectrometry of **Silole-2,5DPA-TRZ**.

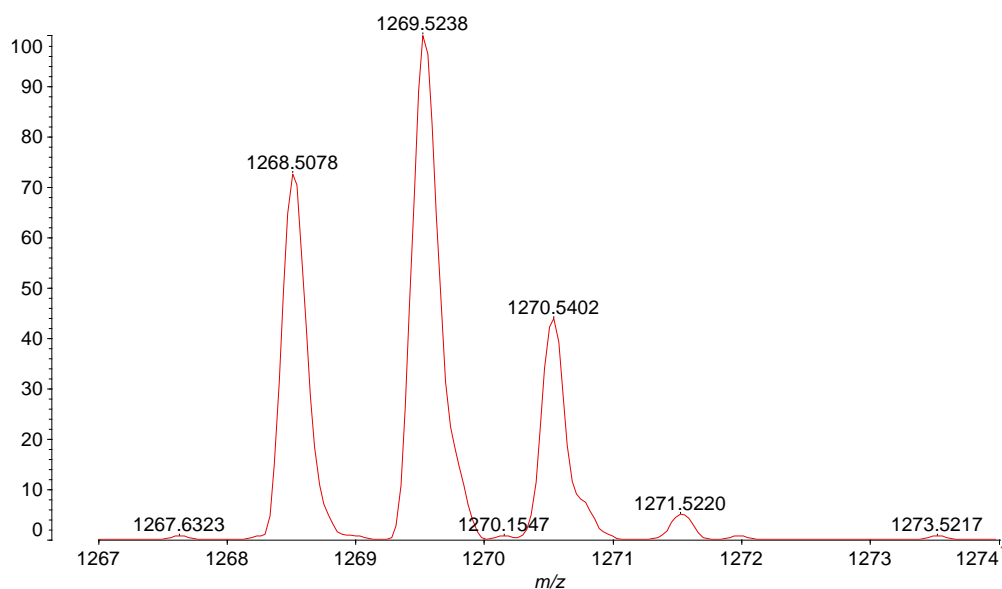


**Figure S12.** MALDI-TOF spectrometry of **Silole-2,5Cz-TRZ**.

### Thermal properties

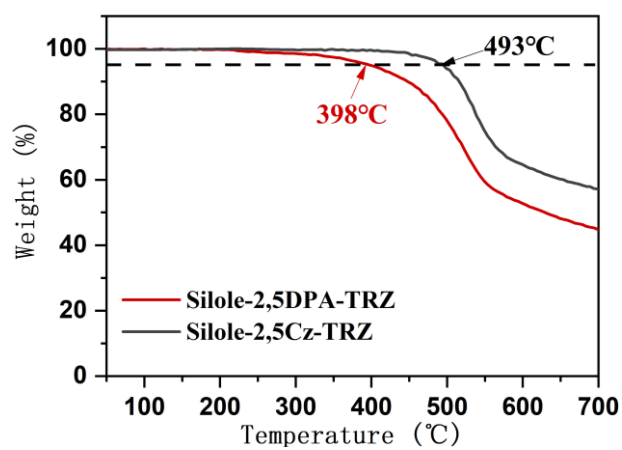


**Figure S13.** The TGA curves of **Silole-2,5DPA-TRZ** and **Silole-2,5Cz-TRZ**.

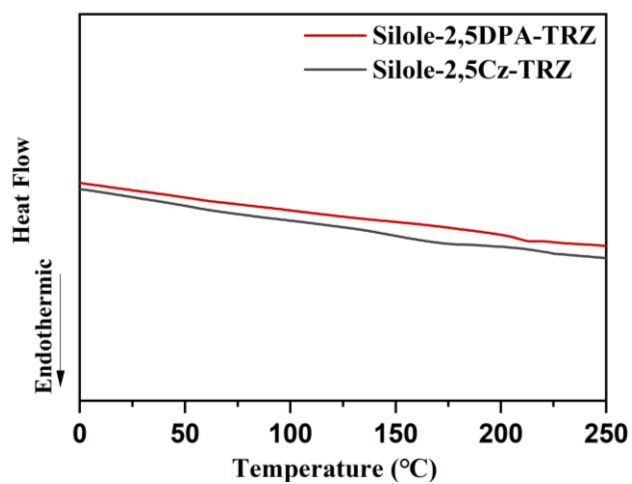


**Figure S14.** The DSC curves of **Silole-2,5DPA-TRZ** and **Silole-2,5Cz-TRZ**.

## Electrochemical Property

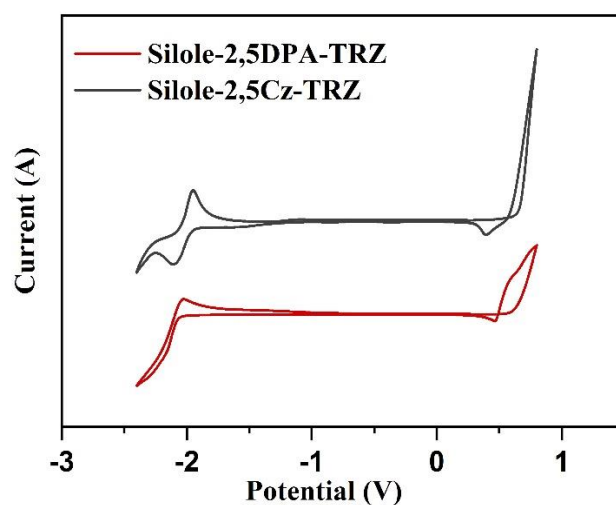


Figure S15. The CV curves of Silole-2,5DPA-TRZ and Silole-2,5Cz-TRZ.

## Photophysical Properties

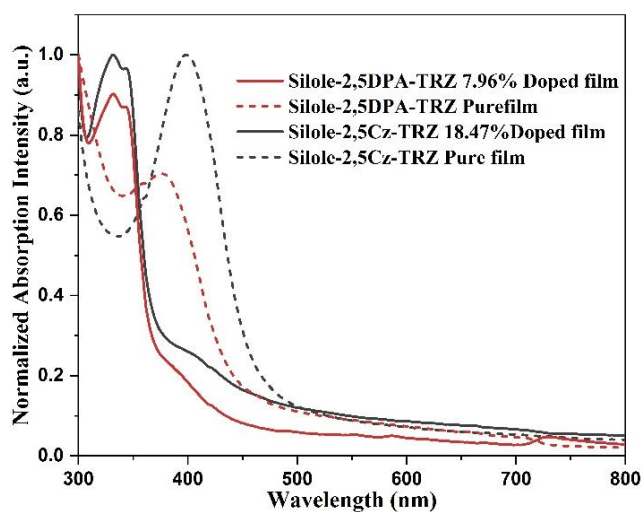
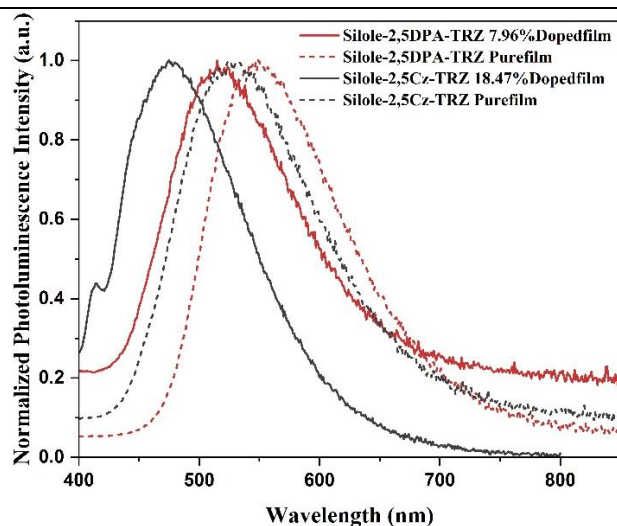
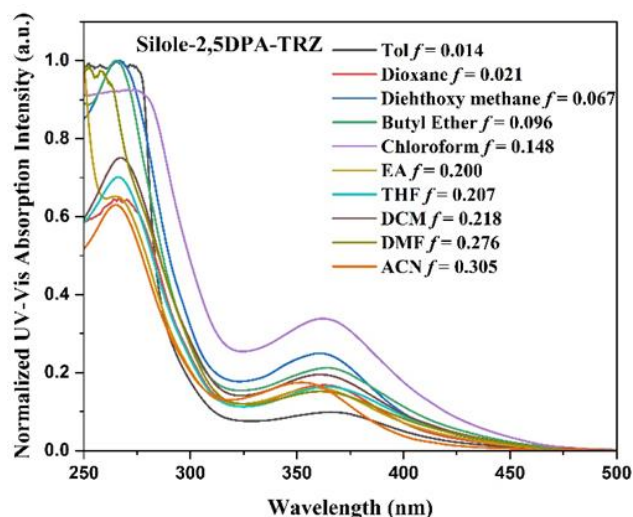


Figure S16. The UV-vis absorption spectra of Silole-2,5DPA-TRZ and Silole-2,5Cz-TRZ in films prepared by thermal deposition (the host material used in the doped film is CBP, doping concentration of Silole-2,5DPA-TRZ: 7.96%, doping concentration of Silole-2,5Cz-TRZ: 18.47%).



**Figure S17.** The PL spectra of **Silole-2,5DPA-TRZ**, **Silole-2,5Cz-TRZ** in films prepared by thermal deposition (the host material used in the doped film is CBP, doping concentration of **Silole-2,5DPA-TRZ**: 7.96%, doping concentration of **Silole-2,5Cz-TRZ**: 18.47%).



**Figure S18.** The UV-Vis absorption spectra of **Silole-2,5DPA-TRZ** in various solvents.

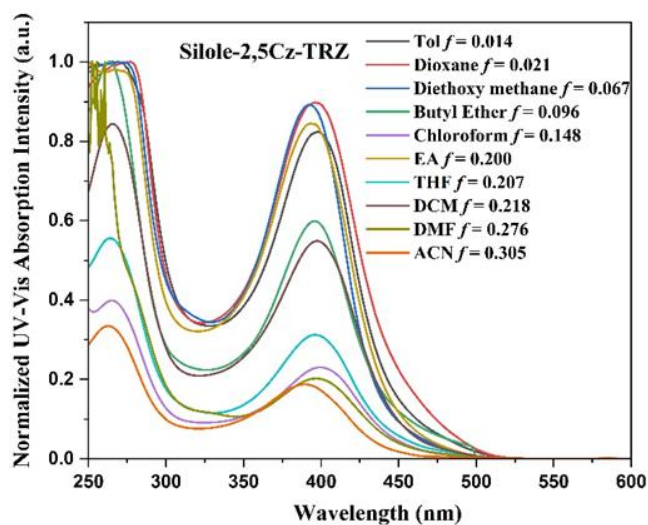


**Figure S19.** The UV-Vis absorption spectra of **Silole-2,5Cz-TRZ** in various solvents.

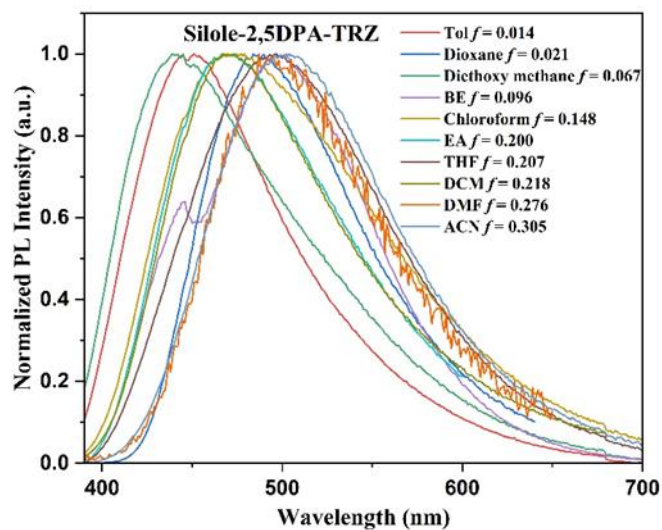


Figure S20. The PL Spectra of Silole-2,5DPA-TRZ in various solvents.

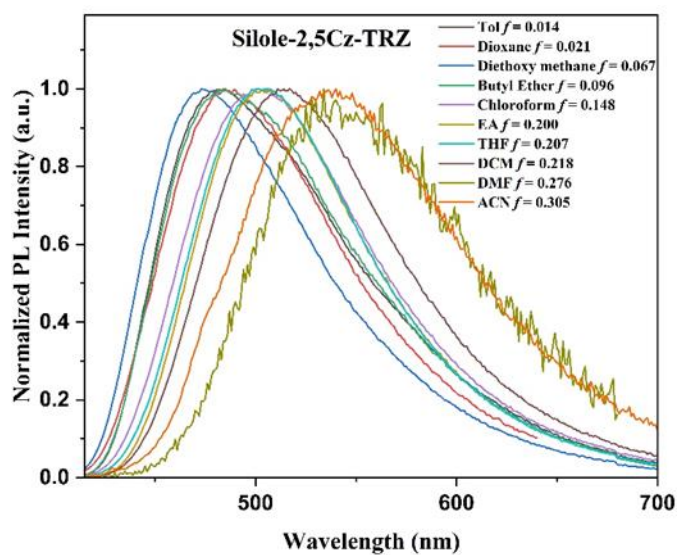


Figure S21. The PL Spectra of Silole-2,5Cz-TRZ in various solvents.

## The solvatochromic Lippert-Mataga model

The influence of solvent environment on the optical property of our compounds can be understood using the Lippert-Mataga equation, [7] a model that describes the interactions between the solvent and the dipole moment of solute:

$$hc(\nu_a - \nu_f) = hc(\nu_a^0 - \nu_f^0) + \frac{1}{4\pi\epsilon_0} \cdot \frac{2(\mu_e - \mu_g)^2}{a^3} f(\epsilon, n) \quad (1)$$

Take differential on both sides of the equation, we got

$$\mu_e = \mu_g + \left\{ \frac{4\pi\epsilon_0 hca^3}{2} \cdot \left[ \frac{d(\nu_a - \nu_f)}{df(\epsilon, n)} \right] \right\}^{\frac{1}{2}} \quad (2)$$

Where  $h$  is the Plank constant,  $c$  is the light speed of light,  $f$  is the orientational polarizability of the solvent,  $\nu_a^0 - \nu_f^0$  corresponds to the Stokes shifts when  $f$  is zero;  $\mu_e$  is the excited state dipole moment,  $\mu_g$  is the ground-state dipole moment;  $a$  is the solvent cavity (Onsager) radius, derived from the Avogadro number ( $N$ ), molecular weight ( $M$ ), and density ( $d=1.0$  g/cm<sup>3</sup>);  $\epsilon_0$  is the permittivity of vacuum;  $\epsilon$  and  $n$  are the solvent dielectric and the solvent refractive index, respectively;  $f(\epsilon, n)$  and  $a$  can be calculated respectively as follows:

$$f(\epsilon, n) = \frac{\epsilon-1}{2\epsilon+1} - \frac{n^2-1}{2n^2+1}, \quad a = (3M/4N\pi d)^{1/3} \quad (3)$$

The differential  $\frac{d(\nu_a - \nu_f)}{df(\epsilon, n)}$  can be estimated with solvatochromic experiment data listed as shown below.

**Table S1.** The wavelength of **Silole-2,5DPA-TRZ** in different solvents

<b>Silole-2,5DPA-TRZ</b>		$\lambda_{\text{abs}}$	$\lambda_{\text{em}}$	$\nu_a - \nu_f$
Solvent	$f(\epsilon, n)$	(nm)	(nm)	(cm <sup>-1</sup> )
Toluene	0.014	365	451	5224
Dioxane	0.021	365	484	6736
Diethoxy methane	0.067	361	439	4921
Butyl Ether (BE)	0.096	364	502	7552
Chloroform	0.148	361	474	6603
EA	0.200	358	467	6519
THF	0.207	363	496	7386
DCM	0.218	361	470	6424
DMF	0.276	360	487	7243
ACN	0.305	353	502	8408

**Table S2.** The wavelength of **Silole-2,5Cz-TRZ** in different solvents

<b>Silole-2,5Cz-TRZ</b>		$\lambda_{\text{abs}}$	$\lambda_{\text{em}}$	$\nu_{\text{a}}-\nu_{\text{f}}$
Solvent	$f(\epsilon, n)$	(nm)	(nm)	( $\text{cm}^{-1}$ )
Toluene	0.014	398	485	4507
Dioxane	0.021	396	484	4591
Diethoxy methane	0.067	393	473	4303
Butyl Ether (BE)	0.096	393	485	4826
Chloroform	0.148	401	500	4937
EA	0.200	394	507	5656
THF	0.207	396	505	5450
DCM	0.218	397	517	5846
DMF	0.276	397	534	6462
ACN	0.305	389	540	7188

### Theoretical calculations

All quantum mechanical calculations were performed using the Gaussian 09 software package.<sup>[8]</sup> The ground state ( $S_0$ ) geometries were optimized at the B3LYP/6-31G(d) level<sup>[9,10]</sup> with the HOMO/LUMO distributions being calculated at the same level based on the optimized  $S_0$  state geometries. The vertical excitation energies of higher energy levels for both singlet and triplet states were calculated using the TD-M062x functional<sup>[11]</sup> and 6-31G(d) basis set starting from the optimized  $S_0$  state geometries. Natural transition orbitals (NTOs)<sup>[12]</sup> involving both singlet and triplet states were evaluated to investigate the properties of the excited states.

Comprehensive electronic excitation characterization of individual excited states was performed using Hole-Electron Analysis<sup>[13-14]</sup> via Multiwfn.<sup>[15]</sup>

### Hole-electron analysis -- IFCT method

The IFCT<sup>[13]</sup> (Inter fragment charge transfer) method calculates the amount of electron transfer from a fragment R to a fragment S during electronic excitation by the following equation:

$$Q_{R,S} = \Theta_{R,\text{hole}} \Theta_{S,\text{ele}} \quad (4)$$

$\Theta_{R,\text{hole}}$  reflects how much of the excited electrons are accounted for by R, and  $\Theta_{S,\text{ele}}$  reflects how much of the place where the electrons are going is accounted for by S. It is clearly reasonable that the product of the two is defined as the amount of electron transfer from R→S. The more holes are accounted for by R, and the more electrons are accounted for by S, then the more R→S is transferred. The inter-fragment charge transfer matrix Q, whose (R,S) element corresponds to the electron transfer from fragment R to fragment S during the excitation process.

After defining the unidirectional electron transfer between fragments as above, we can also define the net electron transfer between two fragments, i.e., the difference between the two directional transfers, as shown in the first equation below. It is then also possible to define the net electron change for a given fragment, i.e., the sum of the net electron transfers between this fragment and all other fragments, as shown in the second equation below:

$$P_{S \rightarrow R} = Q_{S,R} - Q_{R,S} \quad (5)$$

$$\Delta P_R = \sum_{S \neq R} P_{S \rightarrow R} = \sum_{S \neq R} (Q_{S,R} - Q_{R,S}) \quad (6)$$

The diagonal element of the Q matrix in the previous equation is formally the "number of electrons transferred from the fragment to itself", which can be physically interpreted as how many electrons in the fragment are redistributed within the fragment as a result of excitation, and represents the locally excited (LE) state. The off-diagonal element is the "number of electrons transferred between fragments", which represents the charge-transfer (CT) state.

### The Implications of Heat Maps

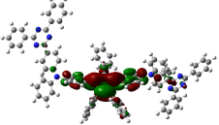
A common way to visualize the size of each matrix element is the heat map, i.e. each grid in the image corresponds to a matrix element, and the grid is colored according to the value of the matrix element, so that it is clear which matrix elements have larger values, and whether they are positive or negative, and the IFCT can be presented in this way as well.

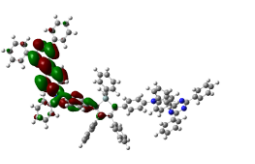
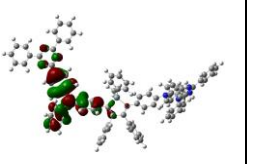
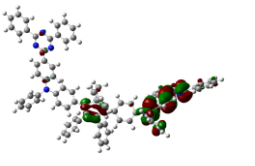
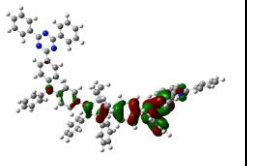
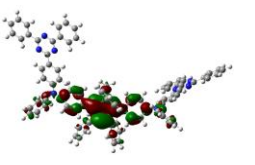
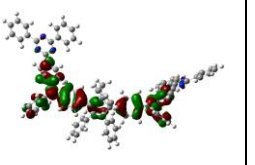
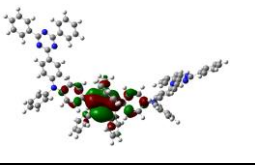
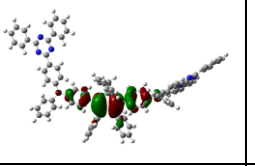
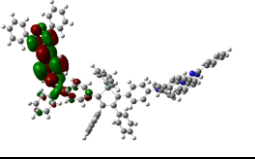
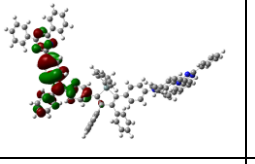
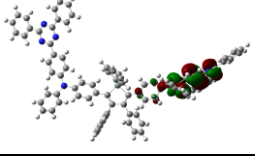
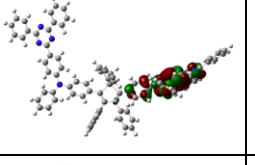
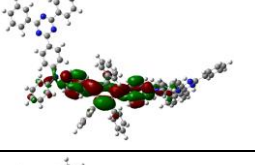
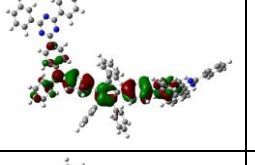
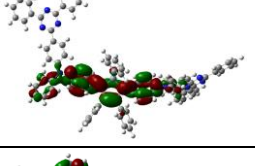
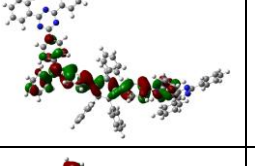
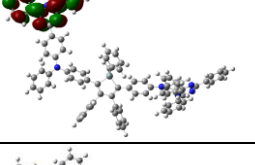
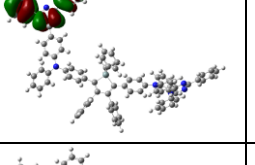
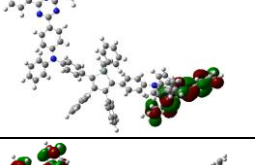
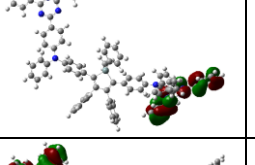
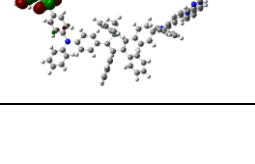
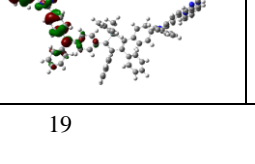
The concepts of charge transfer percentage (CT%) and its complement local excitation percentage (LE%) are frequently involved in electron excitation studies. In the IFCT framework, they can be precisely defined quantitatively. CT% is simply evaluated as  $100\% \times |\Delta P_R|$ , and apparent LE% is defined as  $100\% - \text{CT}\%$ , where R denotes either fragment. The CT% corresponds to the apparent phenomenon of net electron transfer between R and S, namely the cancellation of the bidirectional electron transfer is taken into account.

The molecular orbitals themselves are three-dimensional real-space functions, but defining the basic functions allows them to be represented by the expansion coefficients of the individual basis functions. Similarly, with a particular set of basic functions, the charge transfer (CT) metric is no longer the continuous real-space coordinates  $r$  and  $r'$ , but the ordinal number of the basic functions. With the addition of the corresponding fragment setting, the indicator becomes the fragment number. The heat map of the IFCT was made by replacing the elements in the Q-matrix with colors using the fragment numbers as the horizontal and vertical axes.

According to the idea of the IFCT method, the (I,I) matrix element directly corresponds to the amount of electron redistribution that occurs at the I site during electronic excitation, while the (I,J) matrix element directly corresponds to the number of electrons transferred from the I site to the J site. In the IFCT heatmap, the redder colored part represents a larger amount of electron transfer and conversely the bluer colored portions represent smaller electron transfers.

**Table S3.** NTO and excited state analysis of **Silole-2,5DPA-TRZ** (H: HOMO, L: LUMO)

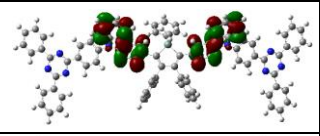
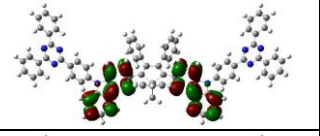
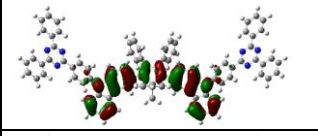
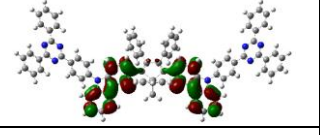
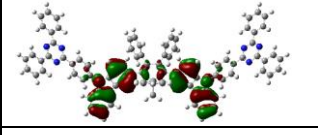
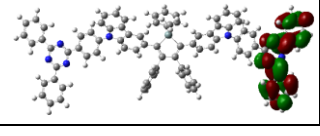
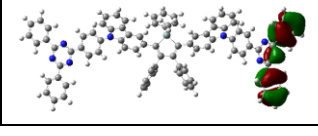
<b>Silole-2,5DPA-TRZ</b>	Main contributing orbitals	Hole	Particle	$f$	$\lambda$ (nm)	CT%	LE%
S <sub>1</sub>	H→L 65.0%, H→L+4 9.4%			1.184	380.93	63.97	36.03

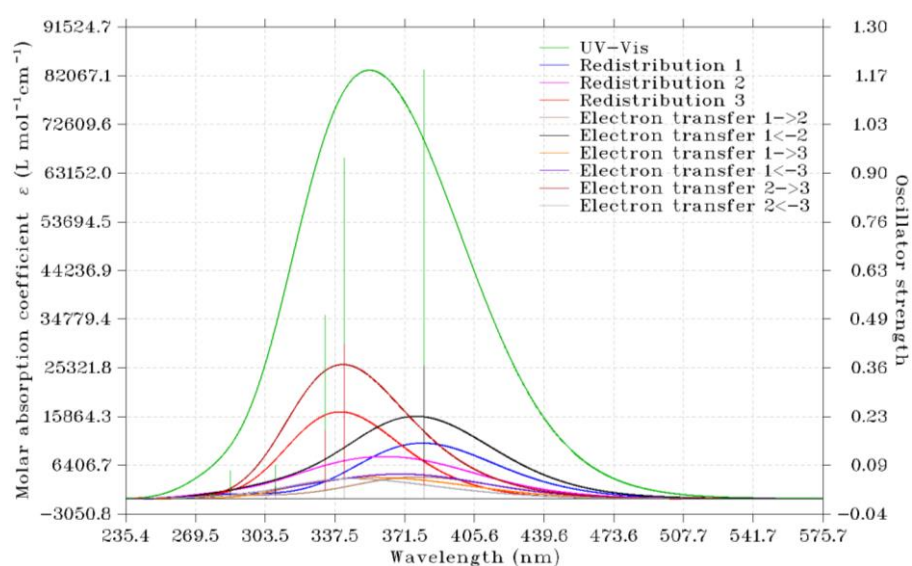
S <sub>2</sub>	H→L+1 39.0%, H-1→L 37.3%			0.942	342.21	60.37	39.63
S <sub>3</sub>	H→L+4 43.9%, H-1→L+1 28.8%			0.506	332.76	66.86	33.14
S <sub>4</sub>	H-1→L+4 42.6%, H-1→L 28.2%			0.001	308.46	69.16	30.84
T <sub>1</sub>	H→L 30.4%, H-2 →L 23.6%			0.000	535.71	34.81	65.19
T <sub>2</sub>	H→L+1 29.1%, H-1→ L 21.6%,			0.000	426.24	45.45	54.56
T <sub>3</sub>	H-1→L+1 25.2%, H→ L+4 15.7%			0.000	423.76	43.79	56.21
T <sub>4</sub>	H-1→L+4 21.7%, H-1→L 16.0%			0.000	367.08	50.52	49.48
T <sub>5</sub>	H→L 9.0%, H-2 →L+4 7.4%,			0.000	350.61	50.32	49.68
T <sub>6</sub>	H-5→L+2 40.3%, H-6→L+2 11.3%			0.000	342.83	4.68	95.32
T <sub>7</sub>	H-4→L+3 46.7%, H-5→L+3 5.2%			0.000	342.60	5.69	94.31
T <sub>8</sub>	H→L+1 39.0%, H-1→L 37.3%			0.000	325.39	8.87	91.13

T <sub>9</sub>	H-7→L+3 25.1%, H-9→L+3 8.1%			0.000	325.26	8.66	91.34
T <sub>10</sub>	H→L+2 13.8%, H-1→L+2 12.1%			0.000	318.01	48.50	51.50

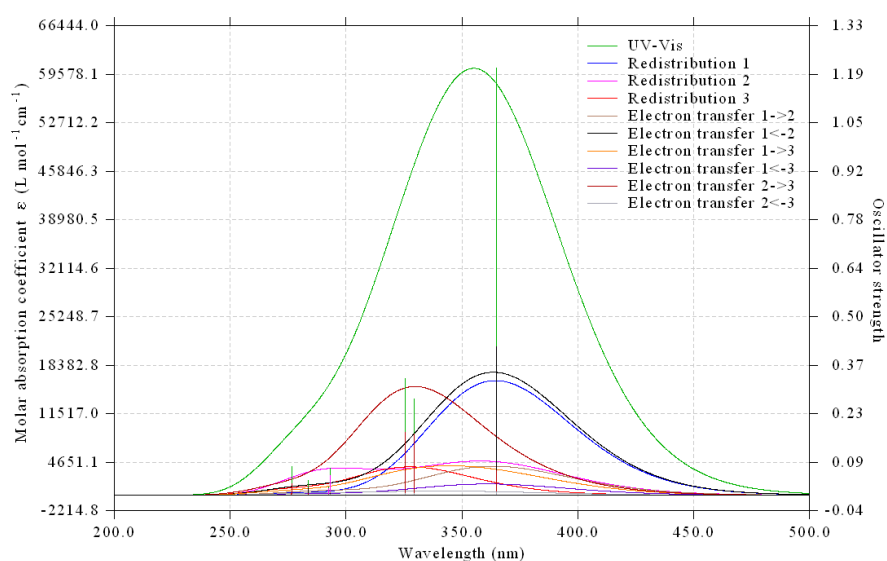
**Table S4.** NTO and excited state analysis of **Silole-2,5Cz-TRZ** (H: HOMO, L: LUMO)

<b>Silole-2,5Cz-TRZ</b>	<i>Main contributing orbitals</i>	<i>Hole</i>	<i>Particle</i>	<i>f</i>	<i>λ (nm)</i>	<i>CT%</i>	<i>LE%</i>
S <sub>1</sub>	H→L+4 68.4%, H→L 16.8%			1.2059	364.75	57.84	42.16
S <sub>2</sub>	H→L+1 51.9%, H-1→L 30.8%			0.2709	329.29	76.35	23.65
S <sub>3</sub>	H→L 37.4%, H-1→L+1 26.2%			0.3305	325.54	78.80	21.20
S <sub>4</sub>	H→L+5 51.2%, H-1→L+6 24.7%			0.0759	293.09	24.83	75.17
T <sub>1</sub>	H→L+4 61.0%, H-4→L+4 17.5%			0.0000	524.93	30.46	69.54
T <sub>2</sub>	H-1→L 24.0%, H→L+1 22.1%			0.0000	383.34	40.38	59.62
T <sub>3</sub>	H-1→L+1 22.5%, H→L 21.3%			0.0000	382.49	37.78	62.22
T <sub>4</sub>	H-1→L+4 18.5%, H-3→L+6 11.6%			0.0000	349.23	53.29	46.71
T <sub>5</sub>	H-11→L+2 19.6%, H-10→L+3 19.6%			0.0000	344.48	21.21	78.79
T <sub>6</sub>	H-11→L+3 16.1%, H-10→L+2 16.1%			0.0000	343.28	32.87	67.13

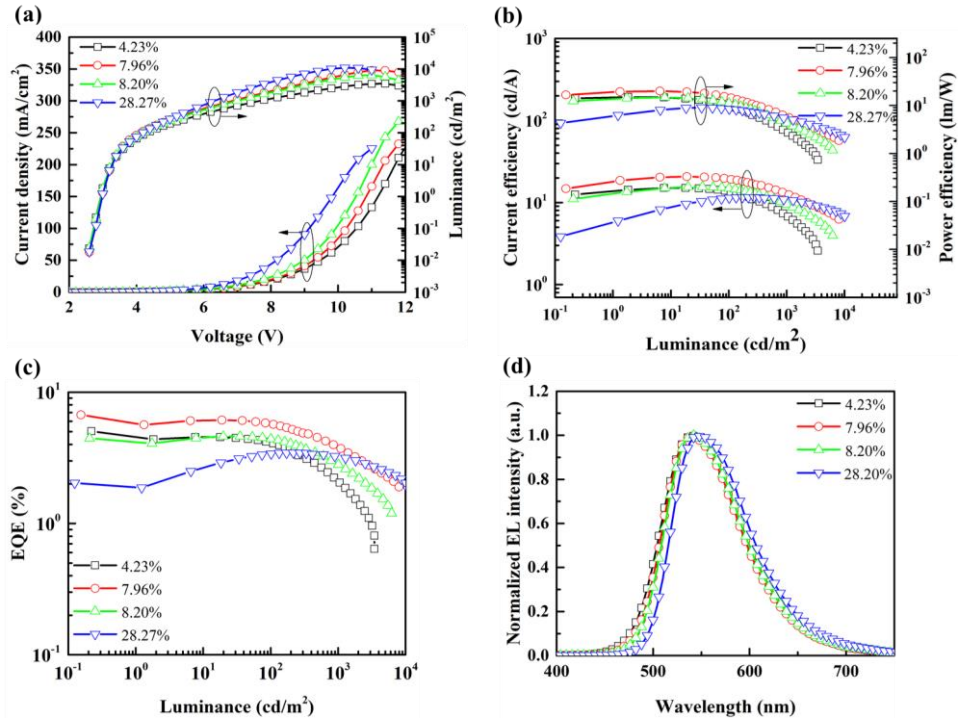
T <sub>7</sub>	H→L+6 36.2%, H-1→L+5 17.7%			0.0000	342.38	19.91	81.09
T <sub>8</sub>	H→L+5 48.4%, H-1→L+6 27.7%			0.0000	342.03	14.68	85.32
T <sub>9</sub>	H-2→L+6 20.5%, H-1→ L+5 16.1%			0.0000	337.62	19,86	80.14
T <sub>10</sub>	H-13→L+2 16.8%, H-12 → L+3 12.7%			0.0000	326.68	0	100



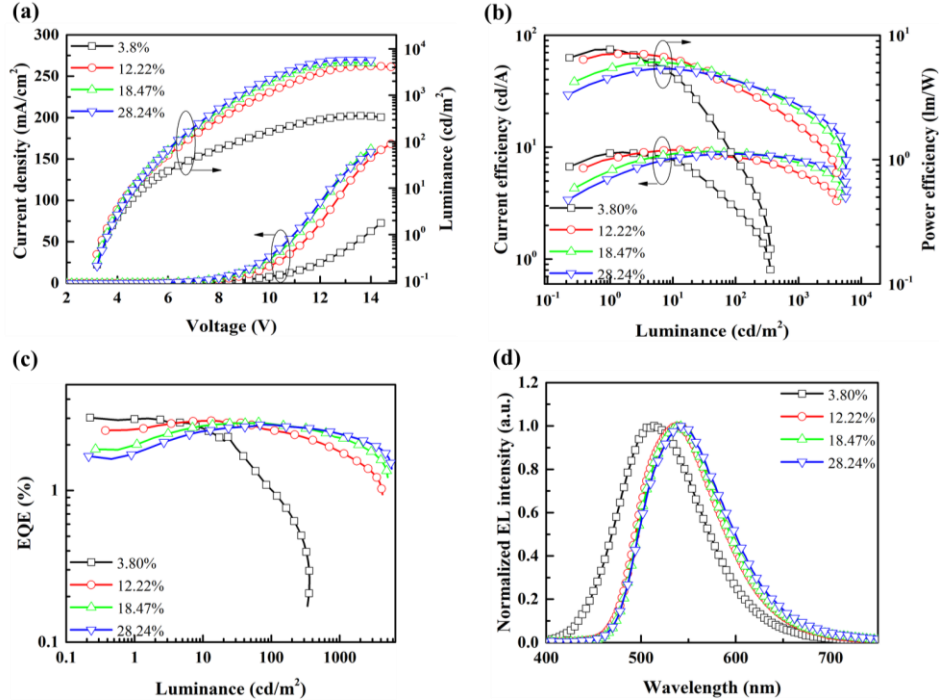
**Figure S22.** The charge transfer spectra of **Silole-2,5DPA-TRZ** (1, 2, 3 represent different segments of silole, DPA, TRZ).



**Figure S23.** The charge transfer spectra of **Silole-2,5Cz-TRZ** (1, 2, 3 represent different segments of silole, Cz, TRZ).



**Figure S24.** Device performance of **Silole-2,5DPA-TRZ** at different doping concentrations (a) current density-voltage-brightness curves; (b) current efficiency-brightness-power efficiency curves; (c) external quantum efficiency-brightness curves; (d) electroluminescence spectra.

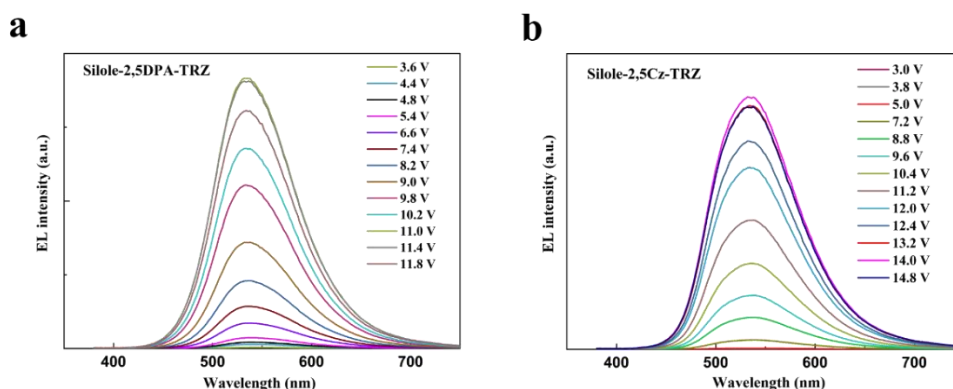
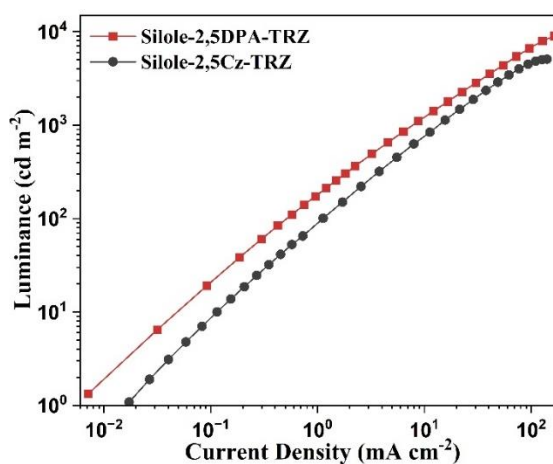


**Figure S25.** Device performance of **Silole-2,5Cz-TRZ** at different doping concentrations (a) current density-voltage-brightness curves; (b) current efficiency-brightness-power efficiency curves; (c) external quantum efficiency-brightness curves; (d) electroluminescence spectra.

**Table S5.** Performance of OLEDs based on **Silole-2,5DPA-TRZ** and **Silole-2,5Cz-TRZ**.

Devices based on different dopants	Dopant Concentration (wt.%)	$V_{on}^a$ (V)	$L_{max}^b$ (cd/m <sup>2</sup> )	$CE_{max}^c$ (cd/A)	$PE_{max}^d$ (lm/W)	$EQE_{max}^e$ (%)	$\lambda_{EL}^f$ (nm)
<b>Silole-2,5DPA-TRZ</b>	4.23	2.9	3461	15.11	15.0	5.04	544
	7.96	2.9	8991	20.72	20.0	6.13	532
	8.20	2.9	6397	15.58	14.75	4.61	542
	28.27	2.9	10930	11.55	9.03	3.45	550
<b>Silole-2,5Cz-TRZ</b>	3.80	3.6	362.3	8.99	7.68	2.26	514
	12.22	3.4	4239	9.45	7.15	2.70	538
	18.47	3.5	5076	9.15	6.07	2.81	540
	28.24	3.6	5762	8.72	5.38	2.72	544

<sup>a</sup>  $V_{on}$ : turn-on voltage at the luminescence of 1 cd m<sup>-2</sup>; <sup>b</sup>  $L_{max}$ : maximum luminance; <sup>c</sup>  $CE_{max}$ : maximum current efficiency; <sup>d</sup>  $PE_{max}$ : maximum power efficiency; <sup>e</sup>  $EQE_{max}$ : maximum EQE; <sup>f</sup>  $\lambda_{EL}$ : maximum emission peak wavelength.

**Figure S26.** EL spectra of devices based on a) **Silole-2,5DPA-TRZ** and b) **Silole-2,5Cz-TRZ** with optimized doping concentrations of 7.96 wt.% and 18.47 wt.% at different driving voltages.**Figure S27.** Luminance-current density relations of best OLEDs based on **Silole-2,5DPA-TRZ** and **Silole-2,5Cz-TRZ**.

---

## Reference

- [1] J. Ohshita, *Macromol. Chem. Phys.*, 2009, **210**, 1360.
- [2] T. Huang, X. Song, M. Cai, D. Zhang, L. Duan, *Materials Today Energy*, 2021, **100705**, 2468.
- [3] P.-W. Long, J.-L. Xie, J.-J. Yang, S.-Q. Lu, Z. Xu, F. Ye, L.-W. Xu, *Chem. Commun.*, 2020, **56**, 4188.
- [4] Y. Chen, D. Zhang, Y. Zhang, X. Zeng, T. Huang, Z. Liu, G. Li, L. Duan, *Adv. Mater.* **2021**, 33, DOI: 10.1002/adma.202103293.
- [5] Z. Yang, Z. Mao, Z. Xie, Y. Zhang, S. Liu, J. Zhao, J. Xu, Z. Chi, M. P. Aldred, *Chem. Soc. Rev.* **2017**, 46, 915.
- [6] H. Uoyama, K. Goushi, K. Shizu, H. Nomura, C. Adachi, *Nature* **2012**, 492, 234.
- [7] a) Z. R. Grabowski, K. Rotkiewicz, W. Rettig, *Chem. Rev.* 2003, **103**, 3899; b) W. Li, D. Liu, F. Shen, D. Ma, Z. Wang, T. Feng, Y. Xu, B. Yang, Y. Ma, *Adv. Funct. Mater.* 2012, **22**, 2797; c) C. Reichardt, T. Welton, *Solvents and Solvent Effects in Organic Chemistry*, Wiley-VCH Verlag & Co. KGaA, Weinheim, Germany 2011, Ch.6.
- [8] Gaussian 09, Revision A.02, M. J. Frisch, G. W. Trucks, H. B. Schlegel, G. E. Scuseria, M. A. Robb, J. R. Cheeseman, G. Scalmani, V. Barone, G. A. Petersson, H. Nakatsuji, X. Li, M. Caricato, A. Marenich, J. Bloino, B. G. Janesko, R. Gomperts, B. Mennucci, H. P. Hratchian, J. V. Ortiz, A. F. Izmaylov, J. L. Sonnenberg, D. Williams-Young, F. Ding, F. Lipparini, F. Egidi, J. Goings, B. Peng, A. Petrone, T. Henderson, D. Ranasinghe, V. G. Zakrzewski, J. Gao, N. Rega, G. Zheng, W. Liang, M. Hada, M. Ehara, K. Toyota, R. Fukuda, J. Hasegawa, M. Ishida, T. Nakajima, Y. Honda, O. Kitao, H. Nakai, T. Vreven, K. Throssell, J. A. Montgomery, Jr., J. E. Peralta, F. Ogliaro, M. Bearpark, J. J. Heyd, E. Brothers, K. N. Kudin, V. N. Staroverov, T. Keith, R. Kobayashi, J. Normand, K. Raghavachari, A. Rendell, J. C. Burant, S. S. Iyengar, J. Tomasi, M. Cossi, J. M. Millam, M. Klene, C. Adamo, R. Cammi, J. W. Ochterski, R. L. Martin, K. Morokuma, O. Farkas, J. B. Foresman, and D. J. Fox, Gaussian, Inc., Wallingford CT, **2016**.
- [9] a) D. Becke, *J. Chem. Phys.* 98 1993, **98**, 5648–5652; b) Lee, W. Yang, R.G. Parr, *Phys. Rev. B.* 1988, **37**, 785; c) H. Vosko, L. Wilk, M. Nusair, *Can. J. Phys.* 1980, **58**, 1200–1211.
- [10] G. A. Petersson, A. Bennett, T. G. Tensfeldt, M. A. Al-Laham, W. A. Shirley, and J. Mantzaris, *J. Chem. Phys.*, 1988, **89**, 2193-218.
- [11] Zhao, D.G. Truhlar, *Theor. Chem. Acc.* 2008, **120**, 215–241.
- [12] NTO R. L. Martin, *J. Chem. Phys.* 2003, **118**, 4775-4777.
- [13] T. Lu, F. W. Chen. *J. Comput. Chem.* 2012, **33**, 580.
- [14] Z. Y. Liu, T. Lu, Qinxue Chen. *Carbon*, 2020, **165**, 461.
- [15] T. Lu, Multiwfn manual Version 3.8(dev), <http://sobereva.com/multiwfn>, Nov. **2023**.